

Weak nonleptonic decays of vector B-mesons

Mikhail A. Ivanov,¹ Zhomart Tyulemissov,^{1,2,3} and Akmaral Tyulemissova^{1,2,3}

¹*Bogoliubov Laboratory of Theoretical Physics,*

Joint Institute for Nuclear Research, Dubna, Russia

²*The Institute of Nuclear Physics,*

Ministry of Energy of the Republic of Kazakhstan, 050032 Almaty, Kazakhstan

³*Al-Farabi Kazakh National University, 050040 Almaty, Kazakhstan*

Abstract

We study the radiative and weak nonleptonic decays of vector B-mesons within the covariant confined quark model (CCQM) developed in our previous papers. First, we calculate the matrix elements and decays widths of the radiative decays $B^* \rightarrow B\gamma$. The obtained results are compared with those obtained in other approaches. Then we consider the nonleptonic decays $B^* \rightarrow D^*V$ which proceed via tree-level quark diagrams. It is shown that the analytical expressions for the amplitudes correspond to the factorization approach. In the framework of our model we calculate the leptonic decay constants and the form factors of the $B^* \rightarrow D^*(V)$ transitions in the entire physical region of the momentum transfer squared. Finally, we calculate the two-body decay widths and compare our results with other models.

I. INTRODUCTION

In 2009, the Belle [1] collaboration has reported on the determination of the masses of the B_s and B_s^* mesons $m_{B_s} = 5364.4 \pm 1.5$ MeV and $m_{B_s^*} = 5416.4 \pm 0.6$ MeV. The LHCb [2] collaboration announced the discovery of a vector B^* -meson with the mass $m(B^*) = 5324.26(41)$ MeV.

Since the $b(c, s, d, u)$ mesons cannot annihilate into gluons, the excited states decay to the ground state via the cascade emission of photons or pion pairs, leading to total widths that are less than a few hundred keV. The difference between masses $m_{B^*} - m_B = 45.21 \pm 0.21$ MeV, a $m_{B_s^*} - m_{B_s} = 48.5_{-1.1}^{+1.8}$ MeV less than the mass of lightest meson (π -meson), ($m_\pi = 134.98$ MeV), as a result of which these mesons cannot decay through a strong channel. Consequently, for vector B -mesons, radiative decays will be dominant. As is known, weak nonleptonic decays of B^* -mesons are always suppressed in comparison with their electromagnetic decay [2]. However, due to small cross sections, these decays have not yet been detected experimentally. The situation can be improved with the help of the LHC and Belle-II experiments, since the annual integrated luminosity of Belle-II is expected to reach $\approx 13 \text{ ab}^{-1}$ and this makes it possible to detect weak decays with branchings greater than $\mathcal{O}(10^{-9})$. Moreover, the LHC experiment will also provide new experimental data for weak decays of B^* -mesons, due to the large production cross section for b -quarks.

A search for excited states of the B_c^\pm -meson has been started at 2014 when the ATLAS collaboration reported on the observation of a new state [3] through its hadronic transition to the ground state B_c^\pm . The mass of the observed state was found to be $6842(6)$ MeV. The mass and decay of this state are consistent with expectations for the second S-wave state of the ground B_c state denoted as $B_c(2^1S_0)$ or $B_c(2S)$. Search for excited B_c^+ states was started at LHCb [4]. In 2019, the CMS collaboration observed two states $B_c(2S)$ and $B_c^*(2S)$ [5] in the $B_c\pi^+\pi^-$ invariant mass spectrum. They are separated in mass by ≈ 29 MeV. The mass of the $B_c(2S)$ is measured to be 6871.0 ± 1.6 MeV. The LHCb collaboration has reported on the observation of an excited B_c state in the $B_c\pi^+\pi^-$ invariant mass spectrum [6]. The observed peak has a mass of 6841.2 ± 1.0 MeV. It is consistent with expectations of the $B_c^*(2^3S_1)$ state. A second state is seen with a mass of 6872.1 ± 1.5 MeV, and is consistent with the $B_c(2^1S_0)$ state.

Radiative and hadronic heavy meson decays of the heavy vector B^* -mesons have been

evaluated using the Heavy Quark Effective Theory and the Vector Meson Dominance hypothesis [7]. It was found that $\Gamma(B^{*+} \rightarrow B^+\gamma) = 220(90)$ eV and $\Gamma(B^{*0} \rightarrow B^0\gamma) = 75(27)$ eV. The radiative and hadronic decays of vector heavy mesons were analyzed within the relativistic quark model with confined light quarks [8]. The following results were obtained for the value of the constituent bottom quark mass $m_b = 5$ GeV, $\Gamma(B^{*+} \rightarrow B^+\gamma) = 401$ eV and $\Gamma(B^{*0} \rightarrow B^0\gamma) = 131$ eV. The method of QCD sum rules in the presence of the external electromagnetic field was used to analyze radiative decays of charmed or bottomed mesons [9]. The calculated values of the decay widths were found to be $\Gamma(B^{*+} \rightarrow B^+\gamma) = 380(60)$ eV, $\Gamma(B^{*0} \rightarrow B^0\gamma) = 130(30)$ eV and $\Gamma(B_s^{*0} \rightarrow B_s^0\gamma) = 220(40)$ eV. Radiative transitions in heavy mesons have been considered in a relativistic quark model [10]. The calculated values of the decay widths with the model parameter $\kappa^q = 0.55$ were found to be $\Gamma(B^{*+} \rightarrow B^+\gamma) = 740(88)$ eV, $\Gamma(B^{*0} \rightarrow B^0\gamma) = 228(27)$ eV, $\Gamma(B_s^{*0} \rightarrow B_s^0\gamma) = 136(12)$ eV. Radiative magnetic dipole decays of heavy-light vector mesons into pseudoscalar mesons have been considered within the relativistic quark model [11]. The results for the mixture of vector and scalar confining potentials with the mixing parameter $\varepsilon = -1$ look as $\Gamma(B^{*+} \rightarrow B^+\gamma) = 190$ eV, $\Gamma(B^{*0} \rightarrow B^0\gamma) = 70$ eV, $\Gamma(B_s^{*0} \rightarrow B_s^0\gamma) = 54$ eV. Decay constants and radiative decays of heavy mesons in light-front quark model [12] were found to be $\Gamma(B^{*+} \rightarrow B^+\gamma) = 400(30)$ eV, $\Gamma(B^{*0} \rightarrow B^0\gamma) = 130(10)$ eV, $\Gamma(B_s^{*0} \rightarrow B_s^0\gamma) = 68(17)$ eV. In this paper [13], the light-front quark model (LFQM) was employed to evaluate the decay widths: $\Gamma(B^{*+} \rightarrow B^+\gamma) = 349(18)$ eV, $\Gamma(B^{*0} \rightarrow B^0\gamma) = 116(6)$ eV, $\Gamma(B_s^{*0} \rightarrow B_s^0\gamma) = 84(10)$ eV. The vector B_c^* meson physics has attracted theorists from all over the world since 1994. First attempt to study B_c^* meson was made in the framework of nonrelativistic quarkonium quantum mechanics by using the QCD-motivated potential [14]. It was found that $\Gamma(B_c^{*+} \rightarrow B_c^+\gamma) = 135$ eV. Later on the authors updated this study and published the new work [15]. In the framework of potential models for heavy quarkonium the mass spectrum for the system $(\bar{b}c)$ was considered [16]. Spin-dependent splittings, taking into account a change of a constant for effective Coulomb interaction between the quarks, and widths of radiative transitions between the $(\bar{b}c)$ levels were calculated $\Gamma(B_c^{*+} \rightarrow B_c^+\gamma) = 60$ eV. In the paper [11], the decay width was found to be $\Gamma(B_c^{*+} \rightarrow B_c^+\gamma) = 33$ eV. The homogeneous bag model was employed in Ref. [17] to calculate the width of the radiative decay $\Gamma(B_c^{*+} \rightarrow B_c^+\gamma) = 53(3)$ eV. The spectrum of heavy mesons including the excited states was treated in the framework of the heavy quark effective theory in Ref. [18]. The

B_c spectroscopy was investigated in a quantum-chromodynamic potential model by using a quantum-chromodynamic potential model [19], within the lattice Non-Relativistic QCD (NRQCD) [20]. Phenomenological predictions of the properties of the B_c system have been done in Ref. [21] by using Richardson's potential. In particular, the width of the radiative decay of B_c^* was found to be $\Gamma(B_c^{*+} \rightarrow B_c^+ \gamma) = 59$ eV. The properties of heavy quarkonia and B_c mesons have been studied in the relativistic quark model [22]. In Ref. [23] the spectrum of the charm-beauty mesons and their radiative decays were studied by using the relativized quark model [23]. It was found that $\Gamma(B_c^{*+} \rightarrow B_c^+ \gamma) = 80$ eV. The observation possibility of B_c excitations at LHC was discussed in Ref. [24].

So far no experimental measurement of the vector B_c^* -meson mass available. However there are a few reliable calculations made in the Lattice QCD. In the paper [25] the prediction was done to be $m(B_c^*) = 6330(7)(2)(6)$ MeV by using the Highly Improved Staggered Quark formalism to handle charm, strange and light valence quarks in full lattice QCD, and NRQCD. The improved results for the B and D meson spectrum from lattice QCD including the effect of u/d , s and c quarks in the sea were presented in Ref. [26]. It was found that $m(B_c^*) = 6278(9)$ MeV. Precise predictions of charmed-bottom hadrons from lattice QCD have been published in Ref. [27], in particularly, $m(B_c^*) = 6331(4)(6)$ MeV.

In the present work we investigate both radiative and weak nonleptonic decays of $B_{(u,d,s,c)}^*$ mesons. We use the covariant confined quark model (CCQM) developed in our previous papers for calculation of the relevant form factors, branching fractions and decay widths. Our paper is organized as follows. In Sec. II we give short sketch to the model and discuss its basic aspects. In Sec. III, we present the detailed calculation of the radiative decays of vector mesons $B^* \rightarrow B\gamma$ in the framework of our approach. Then we give the numerical results for calculated decay widths and compare their values with those obtained in other approaches. In Sec. IV we study the weak nonleptonic decays $B^* \rightarrow D^*V$ where $V = \rho, K^*, D^*, D_s^*$. Since we consider the decays which proceed via tree-level quark diagrams, the matrix elements of two-body decays are factorized into the leptonic decays and the weak meson-meson transition. We calculate the relevant leptonic decay constants and the form factors of those meson-meson transitions in the framework of the CCQM. Finally, we compute the two-body decay widths by using the calculated quantities and compare the obtained results with other approaches. At the end, we make a brief summary of our main results in Sec. V.

II. BASIC ASPECTS OF THE COVARIANT CONFINED QUARK MODEL

The covariant confined quark model is an effective quantum field approach to hadronic interactions based on an interaction Lagrangian of hadrons interacting with their constituent quarks [28]. The coupling strength of the hadrons with the constituent quarks is determined by the so-called compositeness condition $Z_H = 0$ [29, 30] where Z_H is the wave function renormalization constant of the hadron. Matrix elements are generated by a set of quark loop diagrams. The ultraviolet divergences of the quark loops are regularized by including the hadron-quark vertex functions which, in addition, describe finite size effects due to the non-pointlike structure of hadrons. By using Schwinger's α -representation for each local quark propagator and integrating out the loop momenta, one can write the resulting matrix element expression as an integral which includes integrations over a simplex of the α -parameters and an integration over a generalized the Fock-Schwinger proper time. By introducing an infrared cutoff on the upper limit of the proper time one can avoid the appearance of singularities in any matrix element. The new infrared cutoff parameter λ will be taken to have a common value for all processes. The CCQM contains only a few model parameters: the light and heavy constituent quark masses, the size parameters that describe the size of the distribution of the constituent quarks inside the hadron and unified parameter λ . The model parameters are determined by a fit to available experimental data.

The CCQM was successfully applied for description of both light and heavy hadron exclusive decays. In particular, the wide range of the decays of b-hadrons (B , B_s , B_c and Λ_b) have been researched and described [31–42].

In this paper we are going to start with an application of the CCQM to radiative and nonleptonic decays of the vector excited states B^* . An interaction Lagrangian of B -meson which consists from $\bar{q}b$ quarks ($q = u, d, s, c$) are written as

$$\mathcal{L}_{\text{int}} = g_B B(x)J(x) + H.c. \quad (1)$$

The local interpolating current has a form $J = \bar{q}\Gamma b$ where $\Gamma = i\gamma_5$ for a pseudoscalar meson with spin $S = 0$ and $\Gamma = \gamma^\mu$ for a vector meson with spin $S = 1$. The Lorentz index μ is contracting with the corresponding index of a vector state. In the CCQM the nonlocal interpolating currents are used for accounting the internal structure of a hadron. In our case

they are written as

$$J(x) = \int dx_1 \int dx_2 F_B(x, x_1, x_2) \bar{q}_a(x_1) \Gamma b_a(x_2) \quad (2)$$

where $a = 1, 2, 3$ is the color index. The vertex function $F_B(x, x_1, x_2)$ characterizes the finite size of the meson. To satisfy translational invariance the vertex function has to obey the identity $F_B(x + a, x_1 + a, x_2 + a) = F_B(x, x_1, x_2)$ for any given four-vector a . We employ a specific form for the vertex function which satisfies the translation invariance. One has

$$F_B(x, x_1, x_2) = \delta^{(4)}\left(x - \sum_{i=1}^2 w_i x_i\right) \Phi_B\left((x_1 - x_2)^2\right) \quad (3)$$

where Φ_B is the correlation function of the two constituent quarks with masses m_{q_1} and m_{q_2} . The ratios of the quark masses w_i are defined as

$$w_{q_1} = \frac{m_{q_1}}{m_{q_1} + m_{q_2}}, \quad w_{q_2} = \frac{m_{q_2}}{m_{q_1} + m_{q_2}}, \quad w_1 + w_2 = 1. \quad (4)$$

We choose a simple Gaussian form for the Fourier transform of vertex function $\tilde{\Phi}_B(-k^2) = \exp(k^2/\Lambda_B^2)$. The parameter Λ_B characterizes the size of the meson. Since k^2 turns into $-k_E^2$ in Euclidean space the form $\tilde{\Phi}_B(k_E^2)$ has the appropriate fall-off behavior in the Euclidean region.

The coupling constant g_B in Eq. (1) is determined by the so-called *compositeness condition*. The compositeness condition requires that the renormalization constant Z_B of the elementary meson field $B(x)$ is set to zero, i.e.

$$Z_B = 1 - \tilde{\Pi}'_B(p^2) = 0, \quad (p^2 = m_B^2) \quad (5)$$

where $\Pi'_B(p^2)$ is the derivative of the mass function.

S -matrix elements are described by the quark-loop diagrams which are the convolution of the vertex functions and quark propagators. In the evaluation of the quark-loop diagrams we use the local Dirac propagator

$$S_q(k) = \frac{1}{m_q - \not{k} - i\epsilon} = \frac{m_q + \not{k}}{m_q^2 - k^2 - i\epsilon} \quad (6)$$

with an effective constituent quark mass m_q .

The meson functions in the case of the pseudoscalar and vector meson are written as

$$\tilde{\Pi}_P(p^2) = N_c g_P^2 \int \frac{d^4 k}{(2\pi)^4 i} \tilde{\Phi}_P^2(-k^2) \text{tr} \left(\gamma^5 S_1(k + w_1 p) \gamma^5 S_2(k - w_2 p) \right), \quad (7)$$

$$\begin{aligned} \tilde{\Pi}_V^{\mu\nu}(p^2) &= N_c g_V^2 \int \frac{d^4 k}{(2\pi)^4 i} \tilde{\Phi}_V^2(-k^2) \text{tr} \left(\gamma^\mu S_1(k + w_1 p) \gamma^\nu S_2(k - w_2 p) \right) \\ &= g^{\mu\nu} \tilde{\Pi}_V(p^2) + p^\mu p^\nu \tilde{\Pi}_V^\parallel(p^2). \end{aligned} \quad (8)$$

Here $N_c = 3$ is the number of colors. Since the vector meson is on its mass-shell $\epsilon_V \cdot p = 0$ we need to keep the part $\tilde{\Pi}_V(p^2)$. Substituting the derivative of the mass functions into Eq. (5) one can determine the coupling constant g_B as a function of other model parameters. The loop integrations in Eqs. (7) and (8) proceed by using the Fock-Schwinger representation of quark propagators

$$S_q(k + wp) = \frac{1}{m_q - \not{k} - w \not{p}} = (m_q + \not{k} + w \not{p}) \int_0^\infty d\alpha e^{-\alpha[m_q^2 - (k+wp)^2]}. \quad (9)$$

In the obtained integrals over the Fock-Schwinger parameters $0 \leq \alpha_i < \infty$ we introduce an additional integration over the proper time which converts the set of Fock-Schwinger parameters into a simplex. In general case one has

$$\prod_{i=1}^n \int_0^\infty d\alpha_i f(\alpha_1, \dots, \alpha_n) = \int_0^\infty dt t^{n-1} \prod_{i=1}^n \int d\alpha_i \delta \left(1 - \sum_{i=1}^n \alpha_i \right) f(t\alpha_1, \dots, t\alpha_n). \quad (10)$$

Finally, we cut the integration over the proper time at the upper limit by introducing an infrared cutoff λ . One has

$$\int_0^\infty dt(\dots) \rightarrow \int_0^{1/\lambda^2} dt(\dots). \quad (11)$$

This procedure allows us to remove all possible thresholds present in the initial quark diagram. Thus the infrared cutoff parameter λ effectively guarantees the confinement of quarks within hadrons. This method is quite general and can be used for diagrams with an arbitrary number of loops and propagators. In the CCQM the infrared cutoff parameter λ is taken to be universal for all physical processes.

The model parameters are determined by fitting calculated quantities of basic processes to available experimental data or lattice simulations (for details, see Ref. [28]). The numerical values of the constituent quark masses and the cutoff parameter λ are given in Table I.

TABLE I: Model parameters: quark masses and cutoff parameter λ (all in GeV).

m_u	m_s	m_c	m_b	λ
0.241	0.428	1.67	5.04	0.181

III. RADIATIVE DECAYS OF VECTOR B-MESONS

A. $V \rightarrow P\gamma$: theoretical calculation of matrix elements and decay widths

As the first step we consider the radiative decays of vector B^* -mesons. In addition to the strong interaction Lagrangian given by Eq.(1), we need the part describing the electromagnetic interactions. The free Lagrangian of quarks is gauged in the standard manner by using minimal substitution which gives

$$\mathcal{L}_{\text{int}}^{\text{em}}(x) = e A_\mu(x) J_{\text{em}}^\mu(x), \quad J_{\text{em}}^\mu(x) = e_b \bar{b}(x) \gamma^\mu b(x) + e_q \bar{q}(x) \gamma^\mu q(x) \quad (12)$$

where e_b and e_q are the quark charges in units of the positron charge. The radiative decays of a vector mesons into a pseudoscalar meson and photon $V \rightarrow P\gamma$ are described by the Feynman diagrams shown in Fig. 1.

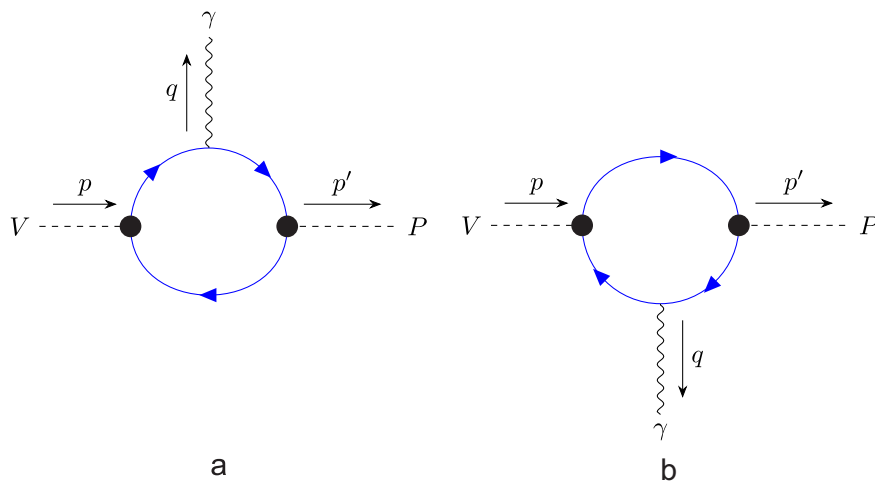


FIG. 1: Feynman diagrams describing the radiative decays of a vector meson.

One has to note that there is an additional piece in the Lagrangian related to the gauging nonlocal interactions of hadrons with their constituents [28]. This piece gives the additional

contributions to the electromagnetic processes. However, they are identically zero for the process $V \rightarrow P\gamma$ due to its anomalous nature.

The matrix element of the process $V \rightarrow P\gamma$ is written down

$$M_{VP\gamma}(p; p', q) = eg_V g_P \epsilon_\nu^V(p) \epsilon_\mu^\gamma(q) \int dx \int dy \int dz e^{-ipx + ip'y + iqz} \langle T \{ \bar{J}_V^\nu(x) J_{\text{em}}^\mu(z) J_P(y) \} \rangle_0. \quad (13)$$

Using the Fourier transforms of the quark currents, we come to the final result

$$\begin{aligned} M_{VP\gamma}(p; p', q) &= (2\pi)^4 i \delta(p - p' - q) M(p, p'), \\ M(p, p') &= (-3i) eg_V g_P \epsilon_\nu^V(p) \epsilon_\mu^\gamma(q) (e_b M_b^{\mu\nu} + e_q M_q^{\mu\nu}) \\ M_b^{\mu\nu} &= \int \frac{dk}{(2\pi)^4 i} \tilde{\Phi}_V(-\ell_1^2) \tilde{\Phi}_P(-\ell_2^2) \text{tr} [S_q(k) \gamma^\nu S_b(k-p) \gamma^\mu S_b(k-p') \gamma^5] \\ M_q^{\mu\nu} &= \int \frac{dk}{(2\pi)^4 i} \tilde{\Phi}_V(-\ell_3^2) \tilde{\Phi}_P(-\ell_4^2) \text{tr} [S_q(k+p') \gamma^\mu S_q(k+p) \gamma^\nu S_b(k) \gamma^5] \end{aligned} \quad (14)$$

where $\ell_1 = k - w_2 p$, $\ell_2 = k - w_2 p'$ and $\ell_3 = k + w_1 p$, $\ell_4 = k + w_1 p'$. The ratios of quark masses are defined by Eq. (4). Now one has $m_{q_1} = m_b$ and $m_{q_2} = m_q$ with $q = u, d, s$. By using the technique of calculations outlined in Sec. II and taking into account the transversality conditions $\epsilon_\mu^\gamma(q) q^\mu = 0$ and $\epsilon_\nu^V(p) p^\nu = 0$ one can arrive at the standard form of matrix element

$$M(p, p') = e g_{VP\gamma} \varepsilon^{pq\mu\nu} \epsilon_\mu^\gamma(q) \epsilon_\nu^V(p), \quad (15)$$

where $g_{VP\gamma} = e_b I_b(m_V^2, m_P^2) + e_q I_q(m_V^2, m_P^2)$ is radiative decay constant. The quantities $I_{b,q}$ are defined by the two-fold integrals which are calculated numerically. The electromagnetic decay width is written as

$$\Gamma(V \rightarrow P + \gamma) = \frac{\alpha}{24} m_V^3 \left(1 - \frac{m_P^2}{m_V^2} \right)^3 g_{VP\gamma}^2. \quad (16)$$

B. $V \rightarrow P\gamma$: numerical results

The masses of the B^* -meson family is not well established yet. We collect the experimentally measured masses of B -meson family in Table II

TABLE II: Masses of B -meson family taken from PDG [43] (in MeV).

B^\pm	B^0	B_s^0	B_c^+	B^*	B_s^*
5279.25(26)	5279.63(20)	5366.91(11)	6274.47(32)	5324.71(21)	5415.8(1.5)

Since the B_c^* or $B_c(1^3S_1)$ state has not been observed yet, we will use the value $m(B_c^*) = 6331(4)(6)$ MeV obtained from lattice QCD [27]. The values of size parameters are taken from our previous papers [40–42]. Their numerical values are given in Table III.

TABLE III: Size parameters of B -meson family (in GeV).

Λ_B	Λ_{B_s}	Λ_{B_c}	Λ_{B^*}	$\Lambda_{B_s^*}$	$\Lambda_{B_c^*}$
1.96	2.05	2.73	1.72	1.71	2.42

The numerical results for the radiative decay constants are shown in Table IV. They are compared with those obtained in Ref. [44].

TABLE IV: The numerical results for the radiative decay constants (in GeV).

$g_{B^{*+}B^+\gamma}$	$g_{B^{*0}B^0\gamma}$	$g_{B_s^{*0}B_s^0\gamma}$	$g_{B_c^{*+}B_c^+\gamma}$	Ref.
1.28(13)	-0.76(8)	-0.57(6)	0.28(3)	CCQM
1.44	-0.91	-0.74	—	[44]

The numerical values for the radiative decay widths are given in Tables V and VI. Our findings are compared with the results obtained in other approaches.

Now, we briefly discuss some error estimates within our model. The CCQM consists of several free parameters: the constituent quark masses m_q , the hadron size parameters Λ_H and the universal infrared cutoff parameter λ . These parameters are determined by minimizing the functional $\chi^2 = \sum_i \frac{(y_i^{\text{expt}} - y_i^{\text{theor}})^2}{\sigma_i^2}$ where σ_i is the experimental uncertainty. If σ is too small then we take its value of 10%. Besides, we have observed that the errors of the fitted parameters are of the order of 10%. Thus, the theoretical error of the CCQM is estimated to be of the order of 10% at the level of matrix elements and the order of 15% at the level of widths.

TABLE V: Widths of $B^* \rightarrow B\gamma$ and $B_s^* \rightarrow B_s\gamma$ decays (in eV).

Mode	CCQM	[13]	[12]	[11]	[10]	[9]	[8]	[7]
$B^{*+} \rightarrow B^+\gamma$	372(56)	349(18)	400(30)	190	740(88)	380(60)	401	220(90)
$B^{*0} \rightarrow B^0\gamma$	126(19)	116(6)	130(10)	70	228(27)	130(30)	131	75(27)
$B_s^{*0} \rightarrow B_s^0\gamma$	90(14)	84(10)	68(17)	54	136(12)	220(40)		

 TABLE VI: Widths of $B_c^* \rightarrow B_c\gamma$ decay (in eV).

Mode	CCQM	[17]	[23]	[21]	[11]	[16]	[14]
$B_c^{*+} \rightarrow B_c^+\gamma$	33(5)	53(3)	80	59	33	60	135

As can be seen from the Table V, there is suppression of the neutral mode $B^{*0} \rightarrow B^0\gamma$ compared to the charged mode $B^{*+} \rightarrow B^+\gamma$. The ratio of those widths is written as

$$\frac{\Gamma(B^{*0} \rightarrow B^0\gamma)}{\Gamma(B^{*+} \rightarrow B^+\gamma)} \sim \frac{(I_b + I_d)^2}{(I_b - 2I_u)^2} \approx 0.38. \quad (17)$$

Note that in the heavy quark limit $m_b \rightarrow \infty$ the integral I_b is suppressed as $1/m_b$ compare with I_q ($q = u, d$). Therefore our result for the ratio in Eq. (17) is not far from the heavy quark limit 0.25. This confirms the observation that the heavy quark limit is quite reliable in the case of b -quark.

IV. NONLEPTONIC DECAYS

The effective Hamiltonian describing the nonleptonic decays $B_{u,d,s}^* \rightarrow D_{u,d,s}^* + V$ where $V = D_{u,d,s}^*, K_{u,d}^*, \rho$ is written down

$$\mathcal{H}_{\text{eff}} = -\frac{G_F}{\sqrt{2}} V_{cb}^* V_{q_1 q_2} \left(C_2 (\bar{c}_a O^\mu b_a) (\bar{q}_{1b} O_\mu q_{2b}) + C_1 (\bar{c}_a O^\mu b_b) (\bar{q}_{1b} O_\mu q_{2a}) \right) \quad (18)$$

where G_F is the Fermi constant, V_{cb} and $V_{q_1 q_2}$ are the matrix elements of the CKM-matrix, C_1 and C_2 is Wilson coefficients and $O^\mu = \gamma^\mu(1 - \gamma_5)$ is the weak matrix with the left chirality. The Wilson coefficients C_2 (leading order) and C_1 (subleading order) are taken at the scale of b -quark mass from Ref. [45] (see, Table 3). One has

$$C_1 = -0.2632 \quad \text{and} \quad C_2 = 1.0111. \quad (19)$$

One has to emphasize that if QCD is neglected, then $C_1 = 0$ and $C_2 = 1$ [46, 47].

We consider the nonleptonic decays $B^* \rightarrow D^*V$ which proceed via tree-level quark diagrams shown in Fig. 2. One has to note that the Wilson coefficients will appear in combinations either $a_1 = C_2 + \xi C_1$ for the charged emitted meson or $a_2 = C_1 + \xi C_2$ for the neutral emitted meson. The color suppression factor $\xi = 1/N_c$ will be used to be equal to zero in calculation that corresponds to the large- N_c limit $\xi = 0$. One has to remind that an approximation is widely used in the phenomenological studies of two-body nonleptonic decays because in the case of $N_c = 3$ the combination $a_2 \approx 0.074$, i.e. significantly suppressed.

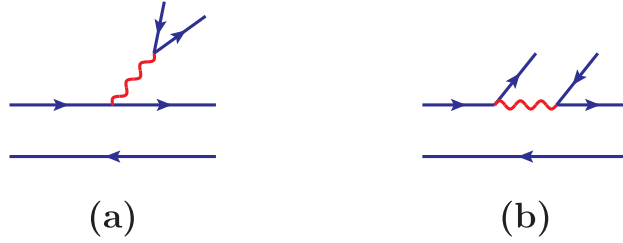


FIG. 2: Tree-level quark diagrams

The Feynman diagram describing the nonleptonic decays $B^* \rightarrow M_1 M_2$ within the CCQM are shown in Fig. 3.

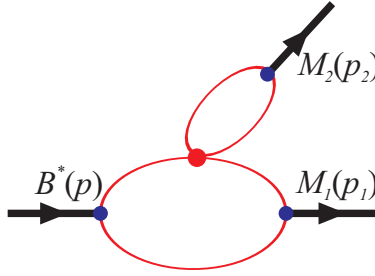


FIG. 3: Diagram describing the nonleptonic decay $B^* \rightarrow M_1 M_2$.

The matrix element of the nonleptonic $B^* \rightarrow M_1(p_1)M_2(p_2)$ decays are given by

$$M(B^*(p) \rightarrow M_1(p_1)M_2(p_2)) = \frac{G_F}{\sqrt{2}} V_{CKM} a_W m_2 f_{M_2} \epsilon_{2\mu} \times \left\langle M_1(p_1, \epsilon_{1\beta}) | \bar{q}_1 O^\mu q_2 | B^*(p, \epsilon_\alpha^*) \right\rangle \quad (20)$$

where f_{M_2} is the leptonic decay constant of the vector meson M_2 . Here V_{CKM} and a_W are the relevant CKM-matrix elements and the Wilson coefficients, respectively. Note that the Eq. (20) is equivalent to the factorization hypothesis.

The leptonic decay constant of the vector meson M_2 which consists from q_1 and q_2 quarks is defined by

$$N_c g_{M_2} \int \frac{d^4 k}{(2\pi)^4 i} \tilde{\Phi}_{M_2}(-k^2) \text{tr} \left[O^\mu S_1(k + w_1 p_2) \not{\epsilon}_2 S_2(k - w_2 p_2) \right] = m_2 f_{M_2} \epsilon_2^\mu. \quad (21)$$

The meson is taken on its mass-shell, i.e. $p_2^2 = m_2^2$ and $\epsilon_2 \cdot p_2 = 0$.

The matrix elements of the weak $B^* - M_1$ transition is written as

$$\begin{aligned} \langle M_1(p_1) | \bar{q}_1 O^\mu q_2 | B^*(p) \rangle = \\ = N_c g_{B^*} g_{M_1} \epsilon_\alpha(p) \epsilon_{1\beta}^*(p_1) \int \frac{d^4 k}{(2\pi)^4 i} \tilde{\Phi}_{B^*} \left(- (k + w_{13} p_1)^2 \right) \tilde{\Phi}_{M_1} \left(- (k + w_{23} p_2)^2 \right) \\ \times \text{tr} \left[O^\mu S_1(k + p_1) \gamma^\alpha S_3(k) \gamma^\beta S_2(k + p_2) \right]. \end{aligned} \quad (22)$$

All particles are on their mass shell: $p^2 = m_{B^*}^2$, $\epsilon_\alpha p^\alpha = 0$, and $p_1^2 = m_1^2$, $\epsilon_{1\beta} p_1^\beta = 0$. Altogether there are three flavors of quarks involved in this process. We therefore introduce a notation with two subscripts $w_{ij} = m_{q_j} / (m_{q_i} + m_{q_j})$ ($i, j = 1, 2, 3$) such that $w_{ij} + w_{ji} = 1$. The loop integrations in the Eqs. (21) and (22) are performed by using technique given in Sec. II. We finalize by two- and three-fold integrals in equations Eqs. (21) and (22), respectively. We calculate them by using FORTRAN codes with NAG library.

The matrix elements of the weak $B^* - M_1$ transition can be expressed in terms of six vector form factors V_i and four axial form factors A_i . One has

$$\begin{aligned} \langle M_1(p_1) | \bar{q}_1 O^\mu q_2 | B^*(p) \rangle = \epsilon_\alpha \epsilon_{1\beta}^* \times \left[g^{\alpha\beta} \left(-P^\mu V_1(q^2) + q^\mu V_2(q^2) \right) \right. \\ \left. + \frac{q^\alpha q^\beta}{M^2 - m_1^2} \left(P^\mu V_3(q^2) - q^\mu V_4(q^2) \right) - q^\alpha g^{\mu\beta} V_5(q^2) + q^\beta g^{\mu\alpha} V_6(q^2) \right] \\ + \epsilon_\alpha \epsilon_{1\beta}^* \times \left[-i \varepsilon^{\mu\nu\alpha\beta} \left(P^\nu A_1(q^2) - q^\nu A_2(q^2) \right) \right. \\ \left. + \frac{i \varepsilon^{\mu\nu\alpha\beta} P^\nu}{M^2 - m_1^2} \left(g^{\nu\alpha} q^\beta A_3(q^2) - g^{\nu\beta} q^\alpha A_4(q^2) \right) \right] \end{aligned} \quad (23)$$

where $P = p + p_1$, $q = p - p_1 = p_2$. The full matrix element of the nonleptonic decay $B^*(p) \rightarrow M_1(p_1) M_2(p_2)$ is obtained by contraction of the above two expressions from Eqs. (21) and (23). Keeping in mind that $\epsilon_2^* \cdot q = (\epsilon_2^* \cdot p_2) = 0$ one gets that the two vector form factors V_2 and V_4 do not contribute to the full matrix element.

The values of the size parameters of vector mesons are taken from Ref. [40–42] and displayed in Table VII.

TABLE VII: Size parameters of vector mesons (in GeV)

Λ_ρ	Λ_{K^*}	Λ_{D^*}	$\Lambda_{D_s^*}$	Λ_{B^*}	$\Lambda_{B_s^*}$
0.61	0.81	1.53	1.56	1.72	1.71

The calculated leptonic decay constants f_{M_2} are shown in Table VIII.

TABLE VIII: Calculated leptonic decay constants f_{M_2} (in MeV)

	CCQM	Expt/Lat
f_ρ	218(22)	221(1) [43]
f_{K^*}	227(23)	217(7) [43]
f_{D^*}	246(25)	223.5(8.4) [48]
$f_{D_s^*}$	273(27)	268.8(6.6) [48]
f_{B^*}	185(19)	186.4(7.1) [48, 49]
$f_{B_s^*}$	260(26)	223.1(5.6) [48, 49]

We calculate the relevant transition form factors in the full kinematical region of the transferred momentum squared q^2 . The behavior of the form factors on the q^2 are shown in Figs. 4-7.

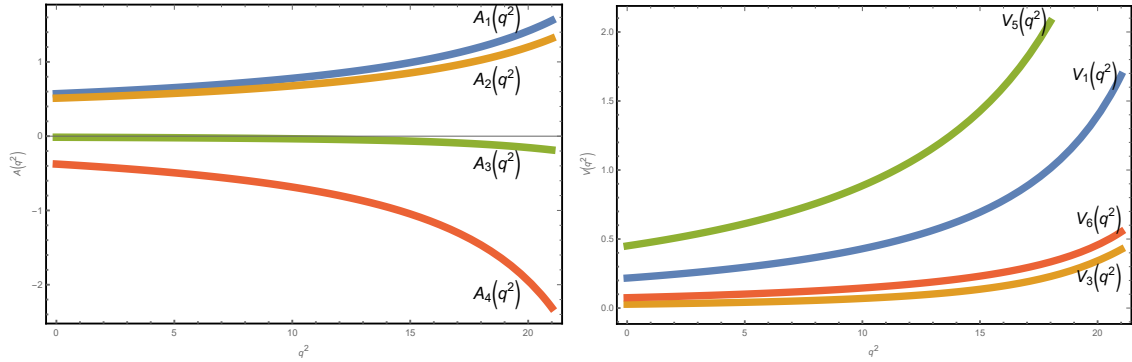


FIG. 4: Form factors of $B^* - \rho$ transition

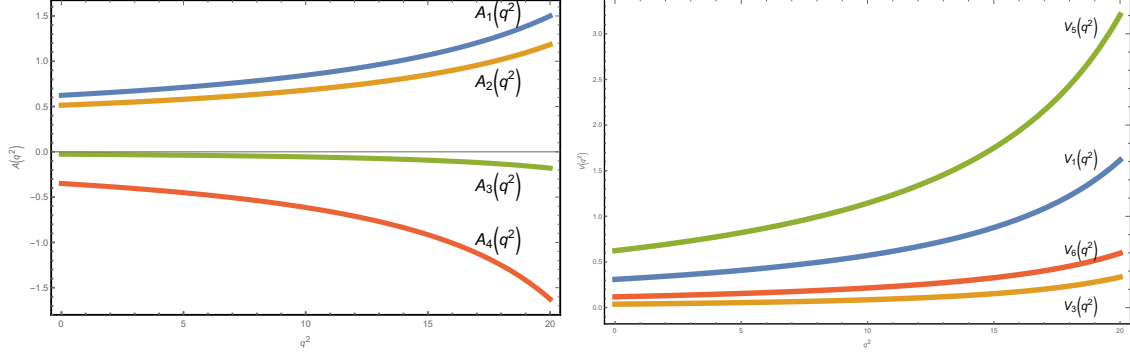


FIG. 5: Form factors of $B^* - K^*$ transition

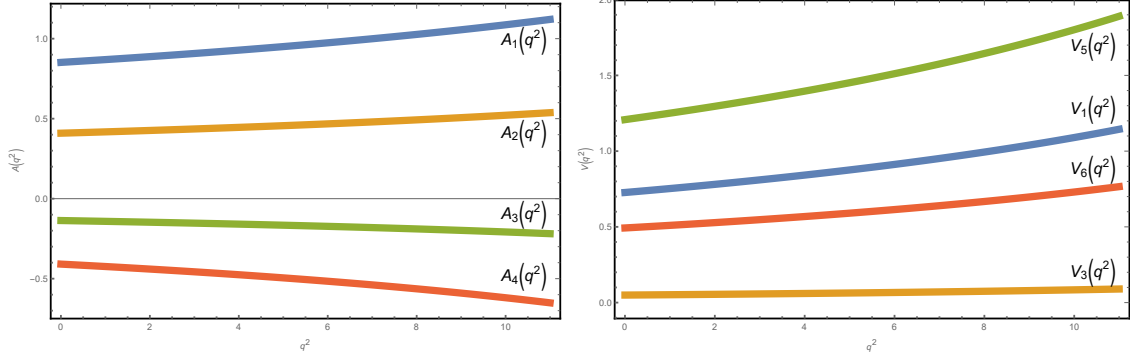


FIG. 6: Form factors of $B^* - D^*$ transition

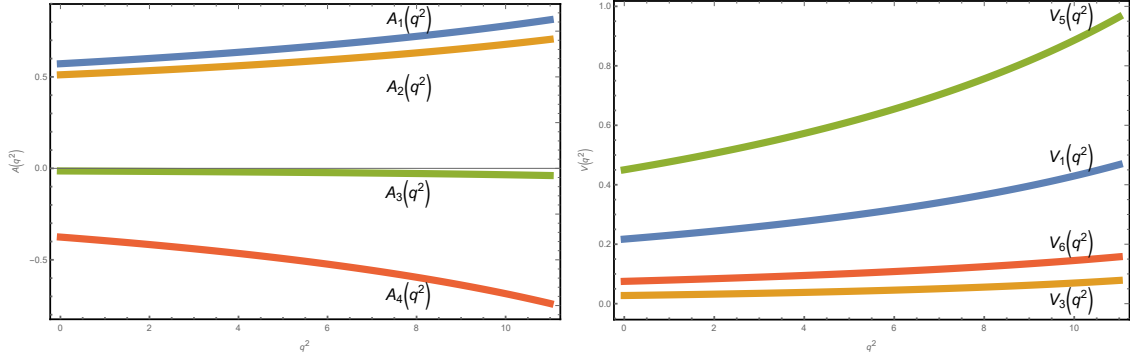


FIG. 7: Form factors of $B_s^* - D_s^*$ transition

The numerical results for the form factors are well approximated by a dipole parametrization

$$F(q^2) = \frac{F(0)}{1 - as + bs^2}, \quad s = \frac{q^2}{M^2} \quad (24)$$

where M is the mass of ingoing meson. The dipole approximation is quite accurate. The error relative to the exact results is less than 1% over the entire q^2 range.

TABLE IX: Parameters of dipole approximation

$B^* - \rho$	A_1	A_2	A_3	A_4	V_1	V_3	V_5	V_6
F(0)	0.57	0.51	-0.014	-0.38	0.22	0.027	0.45	0.075
a	0.66	0.58	2.08	1.42	1.61	2.13	1.59	1.55
b	-0.26	-0.33	1.13	0.39	0.58	1.17	0.57	0.52

$B^* - K^*$	A_1	A_2	A_3	A_4	V_1	V_3	V_5	V_6
F(0)	0.62	0.51	-0.027	-0.35	0.31	0.038	0.62	0.12
a	0.66	0.59	1.75	1.34	1.46	1.92	1.44	1.42
b	-0.24	-0.31	0.77	0.31	0.44	0.94	0.42	0.40

$B^* - D^*$	A_1	A_2	A_3	A_4	V_1	V_3	V_5	V_6
F(0)	0.85	0.41	-0.14	-0.41	0.73	0.050	1.21	0.49
a	0.57	0.56	1.02	1.01	0.98	1.29	0.97	0.95
b	-0.14	-0.15	0.14	0.13	0.11	0.36	0.10	0.089

$B_s^* - D_s^*$	A_1	A_2	A_3	A_4	V_1	V_3	V_5	V_6
F(0)	0.78	0.38	-0.11	-0.34	0.68	0.051	1.16	0.49
a	0.71	0.69	1.16	1.11	1.10	1.36	1.08	1.07
b	-0.13	-0.16	0.21	0.15	0.15	0.38	0.15	0.13

TABLE X: Form factors at origin $q^2 = 0$ compared with CLFQM [13]

$B^* - \rho$	CCQM	CLFQM
A_1	0.57	0.27
A_2	0.51	0.25
A_3	-0.014	0.07
A_4	-0.38	0.06
V_1	0.22	0.28
V_3	0.027	0.11
V_5	0.45	0.60
V_6	0.075	0.14

$B^* - K^*$	CCQM	CLFQM
A_1	0.62	0.33
A_2	0.51	0.27
A_3	-0.027	0.07
A_4	-0.35	0.07
V_1	0.31	0.33
V_3	0.038	0.11
V_5	0.62	0.68
V_6	0.12	0.16

$B^* - D^*$	CCQM	CLFQM
A_1	0.85	0.66
A_2	0.41	0.35
A_3	-0.14	0.07
A_4	-0.41	0.08
V_1	0.73	0.67
V_3	0.050	0.13
V_5	1.21	1.17
V_6	0.49	0.48

$B_s^* \rightarrow D_s^*$	CCQM	CLFQM
A_1	0.78	0.65
A_2	0.38	0.38
A_3	-0.11	0.10
A_4	-0.34	0.09
V_1	0.68	0.66
V_3	0.051	0.15
V_5	1.16	1.19
V_6	0.49	0.53

For convenience of calculation, we further introduce the helicity amplitudes $H_{\lambda_1 \lambda_2}^{M_1 M_2}$ for the outgoing mesons M_1 and M_2 . We imply that the meson M_2 is the emitted meson whereas

M_1 is the outgoing meson in the transition $B^* - M_1$. One has

$$\begin{aligned}
H_{00}^{M_1 M_2} &= f_{M_2} m_2 \left[+ \frac{|\mathbf{p}_2| (M^2 + m_1^2 - m_2^2)}{m_1 m_2} V_1 + \frac{2M^2 |\mathbf{p}_2|^3}{(M^2 - m_1^2) m_1 m_2} V_3 \right. \\
&\quad \left. - \frac{|\mathbf{p}_2| (M^2 - m_1^2 - m_2^2)}{2m_1 m_2} V_5 + \frac{|\mathbf{p}_2| (M^2 - m_1^2 + m_2^2)}{2m_1 m_2} V_6 \right], \\
H_{++}^{M_1 M_2} &= f_{M_2} m_2 \left[+ \frac{3M^2 + m_1^2 - m_2^2}{2M} A_1 - \frac{M^2 - m_1^2 + m_2^2}{2M} A_2 + \frac{2|\mathbf{p}_2|^2 M}{M^2 - m_1^2} A_4 - |\mathbf{p}_2| V_5 \right], \\
H_{--}^{M_1 M_2} &= f_{M_2} m_2 \left[- \frac{3M^2 + m_1^2 - m_2^2}{2M} A_1 + \frac{M^2 - m_1^2 + m_2^2}{2M} A_2 - \frac{2|\mathbf{p}_2|^2 M}{M^2 - m_1^2} A_4 - |\mathbf{p}_2| V_5 \right], \\
H_{+0}^{M_1 M_2} &= f_{M_2} m_2 \left[- \frac{M^2 - m_1^2}{m_2} A_1 + m_2 A_2 + \frac{2M |\mathbf{p}_2|}{m_2} V_1 \right], \\
H_{-0}^{M_1 M_2} &= f_{M_2} m_2 \left[+ \frac{M^2 - m_1^2}{m_2} A_1 - m_2 A_2 + \frac{2M |\mathbf{p}_2|}{m_2} V_1 \right], \\
H_{0-}^{M_1 M_2} &= f_{M_2} m_2 \left[- \frac{M^2 + 3m_1^2 - m_2^2}{2m_1} A_1 + \frac{M^2 - m_1^2 - m_2^2}{2m_1} A_2 - \frac{2|\mathbf{p}_2|^2 M^2}{(M^2 - m_1^2) m_1} A_3 \right. \\
&\quad \left. - \frac{M |\mathbf{p}_2|}{m_1} V_6 \right], \\
H_{0+}^{M_1 M_2} &= f_{M_2} m_2 \left[+ \frac{M^2 + 3m_1^2 - m_2^2}{2m_1} A_1 - \frac{M^2 - m_1^2 - m_2^2}{2m_1} A_2 + \frac{2|\mathbf{p}_2|^2 M^2}{(M^2 - m_1^2) m_1} A_3 \right. \\
&\quad \left. - \frac{M |\mathbf{p}_2|}{m_1} V_6 \right].
\end{aligned}$$

Here $|\mathbf{p}_2| = \lambda^{1/2}(M^2, m_1^2, m_2^2)/2M$ is the momentum of the daughter meson in the B^* -meson rest frame.

Finally, the amplitudes can be written in terms of helicity amplitudes. The only two amplitudes contain the contributions from the diagrams with the charged and neutral emitted mesons. They are written as

$$\begin{aligned}
M(B^{*-} \rightarrow D^{*0} + K^{*-}) &= \frac{G_F}{\sqrt{2}} \left(a_1 V_{cb} V_{us}^* H_{\lambda_{D^*}^* \lambda_{K^*}}^{D^* K^*} + a_2 V_{cb} V_{us}^* H_{\lambda_{K^*}^* \lambda_{D^*}}^{K^* D^*} \right), \\
M(B^{*-} \rightarrow D^{*0} + \rho^-) &= \frac{G_F}{\sqrt{2}} \left(a_1 V_{cb} V_{ud}^* H_{\lambda_{D^*}^* \lambda_{\rho}}^{D^* \rho} + a_2 V_{cb} V_{ud}^* H_{\lambda_{\rho} \lambda_{D^*}}^{\rho D^*} \right). \tag{25}
\end{aligned}$$

Other ten amplitudes contain the contributions from the diagrams with the charged emitted mesons only. One has

TABLE XI: Amplitudes of $B^* \rightarrow D^* V_{\text{charge}}$ decays.

$M(B^* \rightarrow D^* V_{\text{charge}}) = \frac{\mathbf{G_F}}{\sqrt{2}} \mathbf{a_1 V_{cb}} \widetilde{M}(B^* \rightarrow D^* V_{\text{charge}})$			
Mode	\widetilde{M}	Mode	\widetilde{M}
$B^{*-} \rightarrow D^{*0} D^{*-}$	$V_{cd}^* H_{\lambda_{D^{*0}} \lambda_{D^{*-}}}^{D^{*0} D^{*-}}$	$B^{*-} \rightarrow D^{*0} D_s^{*-}$	$V_{cs}^* H_{\lambda_{D^{*0}} \lambda_{D_s^{*-}}}^{D^{*0} D_s^{*-}}$
$\bar{B}^{*0} \rightarrow D^{*+} K^{*-}$	$V_{us}^* H_{\lambda_{D^{*+}} \lambda_{K^{*-}}}^{D^{*+} K^{*-}}$	$\bar{B}^{*0} \rightarrow D^{*+} \rho^-$	$V_{ud}^* H_{\lambda_{D^{*+}} \lambda_{\rho^-}}^{D^{*+} \rho^-}$
$\bar{B}^{*0} \rightarrow D^{*+} D^{*-}$	$V_{cd}^* H_{\lambda_{D^{*+}} \lambda_{D^{*-}}}^{D^{*+} D^{*-}}$	$\bar{B}^{*0} \rightarrow D^{*+} D_s^{*-}$	$V_{cs}^* H_{\lambda_{D^{*+}} \lambda_{D_s^{*-}}}^{D^{*+} D_s^{*-}}$
$\bar{B}_s^{*0} \rightarrow D_s^{*+} K^{*-}$	$V_{us}^* H_{\lambda_{D_s^{*+}} \lambda_{K^{*-}}}^{D_s^{*+} K^{*-}}$	$\bar{B}_s^{*0} \rightarrow D_s^{*+} \rho^-$	$V_{ud}^* H_{\lambda_{D_s^{*+}} \lambda_{\rho^-}}^{D_s^{*+} \rho^-}$
$\bar{B}_s^{*0} \rightarrow D_s^{*+} D^{*-}$	$V_{cd}^* H_{\lambda_{D_s^{*+}} \lambda_{D^{*-}}}^{D_s^{*+} D^{*-}}$	$\bar{B}_s^{*0} \rightarrow D_s^{*+} D_s^{*-}$	$V_{cs}^* H_{\lambda_{D_s^{*+}} \lambda_{D_s^{*-}}}^{D_s^{*+} D_s^{*-}}$

By assuming that the B^* -meson is unpolarized, the decay widths are calculated by the formulas

$$\Gamma(B^{*\lambda} \rightarrow M_1^{\lambda_1} M_2^{\lambda_2}) = \frac{|\mathbf{p_2}|}{24\pi M^2} \sum_{\lambda_1 \lambda_2} |M(B^* \rightarrow M_1 M_2)|^2 \quad (26)$$

where $\lambda = -\lambda_1 + \lambda_2$. In Table XII the branching fractions of all weak nonleptonic decays considered here are given. As wide accepted, we used the calculated values of the radiative decay widths as total widths, i.e. $\Gamma_{\text{tot}}(B^*) = \Gamma(B^* \rightarrow B\gamma)$. For comparison, we give the results obtained in Ref. [13].

TABLE XII: Branching fractions of the $B^* \rightarrow D^*V$ decays ($V = \rho, K^*, D^*, D_s^*$)

Decay mode	CCQM	CLFQM [13]
$B^{*-} \rightarrow D^{*0} + K^{*-}$	$1.02(15) \times 10^{-9}$	$1.10^{+0.01+0.19}_{-0.01-0.17} \times 10^{-11}$
$B^{*-} \rightarrow D^{*0} + \rho^-$	$1.92(29) \times 10^{-8}$	$2.23^{+0.04+0.39}_{-0.04-0.35} \times 10^{-10}$
$B^{*-} \rightarrow D^{*0} + D^{*-}$	$1.75(26) \times 10^{-9}$	$1.44^{+0.11+0.24}_{-0.11-0.22} \times 10^{-11}$
$B^{*-} \rightarrow D^{*0} + D_s^{*-}$	$3.85(58) \times 10^{-8}$	$3.71^{+0.18+0.64}_{-0.18-0.57} \times 10^{-10}$
$\bar{B}^{*0} \rightarrow D^{*+} + K^{*-}$	$4.62(69) \times 10^{-9}$	$3.40^{+0.24+0.58}_{-0.23-0.52} \times 10^{-11}$
$\bar{B}^{*0} \rightarrow D^{*+} + \rho^-$	$8.09(1.21) \times 10^{-8}$	$6.85^{+0.26+1.17}_{-0.26-1.05} \times 10^{-10}$
$\bar{B}^{*0} \rightarrow D^{*+} + D^{*-}$	$5.12(77) \times 10^{-9}$	$4.33^{+0.33+0.74}_{-0.32-0.66} \times 10^{-11}$
$\bar{B}^{*0} \rightarrow D^{*+} + D_s^{*-}$	$1.17(18) \times 10^{-7}$	$1.11^{+0.06+0.19}_{-0.05-0.17} \times 10^{-9}$
$\bar{B}_s^{*0} \rightarrow D_s^{*+} + K^{*-}$	$5.63(84) \times 10^{-9}$	$4.80^{+0.34+0.83}_{-0.32-0.74} \times 10^{-11}$
$\bar{B}_s^{*0} \rightarrow D_s^{*+} + \rho^-$	$5.21(78) \times 10^{-9}$	$9.39^{+0.36+1.63}_{-0.35-1.46} \times 10^{-10}$
$\bar{B}_s^{*0} \rightarrow D_s^{*+} + D^{*-}$	$6.51(98) \times 10^{-9}$	$6.10^{+0.47+1.03}_{-0.45-0.92} \times 10^{-11}$
$\bar{B}_s^{*0} \rightarrow D_s^{*+} + D_s^{*-}$	$1.48(22) \times 10^{-7}$	$1.54^{+0.08+0.26}_{-0.07-0.24} \times 10^{-9}$

One can see from Table XII that our results are almost two order larger in magnitude than those from Ref. [13]. Unfortunately, the authors of [13] did not give the numerical coefficients for the Wilson coefficients C_1 and C_2 , there are only the combinations of $\alpha_1 = C_1 + \xi C_2$ and $\alpha_2 = C_2 + \xi C_1$ with $\xi = 1/N_c$. However, they refer to the papers by Buras et al. [46, 47] in which the notation are accepted as $C_2 = 1$ and $C_1 = 0$ if QCD is neglected. We are using the Wilson coefficients from Ref. [45] (see, Table 3, and references therein) where their values have been calculated by using the various corrections and found that $C_1 = -0.2632$ and $C_2 = 1.0111$. If one uses these values for α_1 and α_2 of Ref. [13] then one arrives at $\alpha_1 \approx 0.074$ for $N_c = 3$, i.e. strongly suppressed, whereas the value of $\alpha_2 = 0.923$ is of the leading order. If compare the analytical expressions for the decay amplitudes from [13] (see, Eqs. (13)-(24)) with our results given by Eq. 25 and Table XI, then one finds that in Ref. [13] the amplitudes with the charged emitted mesons are proportional to α_1 which is suppressed whereas in our approach those amplitudes are proportional to $a_1 = C_2 + \xi C_1$ which is of leading order. It could explain two order difference for branching fractions obtained in these

two approaches.

V. SUMMARY

The radiative and weak nonleptonic decays of vector B -mesons have been studied within the covariant confined quark model (CCQM) developed in our previous papers. The matrix elements and decays widths of the radiative decays $B^* \rightarrow B\gamma$ were calculated. The obtained results were compared with those obtained in other approaches.

The nonleptonic decays $B^* \rightarrow D^*V$ which proceed via tree-level quark diagrams have been carefully analyzed. It was shown that the analytical expressions for the amplitudes correspond to the factorization approach. In the framework of our approach we calculated the leptonic decay constants and the form factors of the $B^* \rightarrow D^*(V)$ transitions in the entire physical region of the momentum transfer squared. Finally, we calculated the two-body decay widths and compared our results with other models.

VI. ACKNOWLEDGEMENTS

This work is supported by the JINR grant of young scientists and specialists No. 22-302-06. Zh.T.'s research has been funded by the Science Committee of the Ministry of Education and Science of the Republic of Kazakhstan (Grant No. AP09057862).

-
- [1] R. Louvot *et al.* [Belle], Phys. Rev. Lett. **102**, 021801 (2009) [arXiv:0809.2526 [hep-ex]].
 - [2] R. Aaij *et al.* [LHCb], Phys. Rev. Lett. **110**, no.15, 151803 (2013) [arXiv:1211.5994 [hep-ex]].
 - [3] G. Aad *et al.* [ATLAS], Phys. Rev. Lett. **113**, no.21, 212004 (2014) [arXiv:1407.1032 [hep-ex]].
 - [4] R. Aaij *et al.* [LHCb], JHEP **01**, 138 (2018) [arXiv:1712.04094 [hep-ex]].
 - [5] A. M. Sirunyan *et al.* [CMS], Phys. Rev. Lett. **122**, no.13, 132001 (2019) [arXiv:1902.00571 [hep-ex]].
 - [6] R. Aaij *et al.* [LHCb], Phys. Rev. Lett. **122**, no.23, 232001 (2019) [arXiv:1904.00081 [hep-ex]].
 - [7] P. Colangelo, F. De Fazio and G. Nardulli, Phys. Lett. B **316**, 555-560 (1993) [arXiv:hep-ph/9307330 [hep-ph]].
 - [8] M. A. Ivanov and Y. M. Valit, Z. Phys. C **67**, 633-640 (1995)

- [9] S. L. Zhu, W. Y. P. Hwang and Z. s. Yang, Mod. Phys. Lett. A **12**, 3027-3036 (1997) [arXiv:hep-ph/9610412 [hep-ph]].
- [10] J. L. Goity and W. Roberts, Phys. Rev. D **64**, 094007 (2001) [arXiv:hep-ph/0012314 [hep-ph]].
- [11] D. Ebert, R. N. Faustov and V. O. Galkin, Phys. Lett. B **537**, 241-248 (2002) [arXiv:hep-ph/0204089 [hep-ph]].
- [12] H. M. Choi, Phys. Rev. D **75**, 073016 (2007) [arXiv:hep-ph/0701263 [hep-ph]].
- [13] Q. Chang, Y. Zhang and X. Li, Chin. Phys. C **43**, no.10, 103104 (2019) [arXiv:1908.00807 [hep-ph]].
- [14] E. J. Eichten and C. Quigg, Phys. Rev. D **49**, 5845-5856 (1994) [arXiv:hep-ph/9402210 [hep-ph]].
- [15] E. J. Eichten and C. Quigg, Phys. Rev. D **99**, no.5, 054025 (2019) [arXiv:1902.09735 [hep-ph]].
- [16] S. S. Gershtein, V. V. Kiselev, A. K. Likhoded and A. V. Tkabladze, Phys. Rev. D **51**, 3613-3627 (1995) [arXiv:hep-ph/9406339 [hep-ph]].
- [17] C. W. Liu and B. D. Wan, Phys. Rev. D **105**, no.11, 114015 (2022) [arXiv:2204.08207 [hep-ph]].
- [18] J. Zeng, J. W. Van Orden and W. Roberts, Phys. Rev. D **52**, 5229-5241 (1995) [arXiv:hep-ph/9412269 [hep-ph]].
- [19] S. N. Gupta and J. M. Johnson, Phys. Rev. D **53**, 312-314 (1996) [arXiv:hep-ph/9511267 [hep-ph]].
- [20] C. T. H. Davies, K. Hornbostel, G. P. Lepage, A. J. Lidsey, J. Shigemitsu and J. H. Sloan, Phys. Lett. B **382**, 131-137 (1996) [arXiv:hep-lat/9602020 [hep-lat]].
- [21] L. P. Fulcher, Phys. Rev. D **60**, 074006 (1999) [arXiv:hep-ph/9806444 [hep-ph]].
- [22] D. Ebert, R. N. Faustov and V. O. Galkin, Phys. Rev. D **67**, 014027 (2003) [arXiv:hep-ph/0210381 [hep-ph]].
- [23] S. Godfrey, Phys. Rev. D **70**, 054017 (2004) [arXiv:hep-ph/0406228 [hep-ph]].
- [24] A. Berezhnoy and A. Likhoded, PoS **QFTHEP2013**, 051 (2013) [arXiv:1307.5993 [hep-ph]].
- [25] E. B. Gregory, C. T. H. Davies, E. Follana, E. Gamiz, I. D. Kendall, G. P. Lepage, H. Na, J. Shigemitsu and K. Y. Wong, Phys. Rev. Lett. **104**, 022001 (2010) [arXiv:0909.4462 [hep-lat]].
- [26] R. J. Dowdall, C. T. H. Davies, T. C. Hammant and R. R. Horgan, Phys. Rev. D **86**, 094510 (2012) [arXiv:1207.5149 [hep-lat]].

- [27] N. Mathur, M. Padmanath and S. Mondal, Phys. Rev. Lett. **121**, no.20, 202002 (2018) [arXiv:1806.04151 [hep-lat]].
- [28] T. Branz, A. Faessler, T. Gutsche, M. A. Ivanov, J. G. Körner and V. E. Lyubovitskij, Phys. Rev. D **81**, 034010 (2010) [arXiv:0912.3710 [hep-ph]].
- [29] A. Salam, Nuovo Cim. **25**, 224-227 (1962)
- [30] S. Weinberg, Phys. Rev. **130**, 776-783 (1963)
- [31] M. A. Ivanov, J. G. Körner and P. Santorelli, Phys. Rev. D **73**, 054024 (2006) [arXiv:hep-ph/0602050 [hep-ph]].
- [32] M. A. Ivanov, J. G. Körner and P. Santorelli, Phys. Rev. D **63**, 074010 (2001) [arXiv:hep-ph/0007169 [hep-ph]].
- [33] A. Faessler, T. Gutsche, M. A. Ivanov, J. G. Körner and V. E. Lyubovitskij, Eur. Phys. J. direct **4**, no.1, 18 (2002) [arXiv:hep-ph/0205287 [hep-ph]].
- [34] T. Gutsche, M. A. Ivanov, J. G. Körner, V. E. Lyubovitskij, P. Santorelli and N. Haby, Phys. Rev. D **91**, no.7, 074001 (2015) [erratum: Phys. Rev. D **91**, no.11, 119907 (2015)] [arXiv:1502.04864 [hep-ph]].
- [35] M. A. Ivanov, J. G. Körner and P. Santorelli, Phys. Rev. D **71**, 094006 (2005) [erratum: Phys. Rev. D **75**, 019901 (2007)] [arXiv:hep-ph/0501051 [hep-ph]].
- [36] M. A. Ivanov, J. G. Körner and C. T. Tran, Phys. Rev. D **94**, no.9, 094028 (2016) [arXiv:1607.02932 [hep-ph]].
- [37] C. T. Tran, M. A. Ivanov, J. G. Körner and P. Santorelli, Phys. Rev. D **97**, no.5, 054014 (2018) [arXiv:1801.06927 [hep-ph]].
- [38] M. A. Ivanov, J. G. Körner and O. N. Pakhomova, Phys. Lett. B **555**, 189-196 (2003) [arXiv:hep-ph/0212291 [hep-ph]].
- [39] A. Issadykov and M. A. Ivanov, Phys. Lett. B **783**, 178-182 (2018) [arXiv:1804.00472 [hep-ph]].
- [40] S. Dubnicka, A. Z. Dubnickova, A. Issadykov, M. A. Ivanov and A. Liptaj, Phys. Rev. D **96**, no.7, 076017 (2017) [arXiv:1708.09607 [hep-ph]].
- [41] T. Gutsche, M. A. Ivanov, J. G. Körner and V. E. Lyubovitskij, Phys. Rev. D **98**, no.7, 074011 (2018) [arXiv:1806.11549 [hep-ph]].
- [42] M. A. Ivanov, J. G. Körner, J. N. Pandya, P. Santorelli, N. R. Soni and C. T. Tran, Front. Phys. (Beijing) **14**, no.6, 64401 (2019) [arXiv:1904.07740 [hep-ph]].
- [43] R. L. Workman *et al.* [Particle Data Group], PTEP **2022**, 083C01 (2022)

doi:10.1093/ptep/ptac097

- [44] H. D. Li, C. D. Lü, C. Wang, Y. M. Wang and Y. B. Wei, JHEP **04**, 023 (2020) [arXiv:2002.03825 [hep-ph]].
- [45] S. Descotes-Genon, T. Hurth, J. Matias and J. Virto, JHEP **05**, 137 (2013) [arXiv:1303.5794 [hep-ph]].
- [46] G. Buchalla, A. J. Buras and M. E. Lautenbacher, Rev. Mod. Phys. **68**, 1125-1144 (1996) [arXiv:hep-ph/9512380 [hep-ph]].
- [47] A. J. Buras, [arXiv:hep-ph/9806471 [hep-ph]].
- [48] V. Lubicz *et al.* [ETM], Phys. Rev. D **96**, no.3, 034524 (2017) [arXiv:1707.04529 [hep-lat]].
- [49] A. Bussone *et al.* [ETM], Phys. Rev. D **93**, no.11, 114505 (2016) [arXiv:1603.04306 [hep-lat]].